Crystal structure of the mineral strontiodresserite from laboratory powder diffraction data

P. S. Whitfield[a)]
Institute for Chemical Process and Environmental Technology, National Research Council Canada, 1200 Montreal Road, Ottawa, Ontario K1A 0R6, Canada

L. D. Mitchell
Institute for Research in Construction, National Research Council Canada, 1200 Montreal Road, Ottawa, Ontario K1A 0R6, Canada

Y. Le Page
Institute for Chemical Process and Environmental Technology, National Research Council Canada, 1200 Montreal Road, Ottawa, Ontario K1A 0R6, Canada

J. Margeson
Institute for Research in Construction, National Research Council Canada, 1200 Montreal Road, Ottawa, Ontario K1A 0R6, Canada

A. C. Roberts
Geological Survey of Canada, 601 Booth Street, Ottawa, Ontario K1A 0E8, Canada

(Received 9 June 2010; accepted 16 September 2010)

The crystal structure of the mineral strontiodresserite, $(Sr,Ca)Al_2(CO_3)_2(OH)_4 \cdot H_2O$, from the Francon Quarry, Montreal, Quebec, Canada, has been solved from laboratory powder diffraction data using a combination of charge-flipping and simulated annealing methods. The structure is orthorhombic in space group *Pnma* with $a=16.0990(7)$, $b=5.6133(3)$, and $c=9.1804(4)$ Å ($Z=4$) and the framework of the mineral is isostructural with that of dundasite. The strontium has a coordination number of 9 and the carbonate anions form a bridge between the SrO_9 polyhedra and AlO_6 octahedra. The water molecule lies in a channel that runs parallel to the *b* axis. An ordered network of hydrogen atoms could be uniquely determined from crystal-chemical principles in the channels of strontiodresserite. *Ab initio* density functional theory (DFT) energy minimization of the whole structure gave results in full agreement with X-ray refinement results for nonhydrogen atoms. The stability of this model (as well as that of the corresponding model of dundasite) in the proposed *Pnma* space group was tested by DFT optimization in space group *P*1 of random small distortions of this structure. This test confirms that both minerals are isostructural, including their hydrogen-bond networks.
[DOI: 10.1154/1.3504496]

Key words: mineral, charge flipping, simulated annealing, Rietveld refinement

I. INTRODUCTION

Strontiodresserite is a hydrated strontium-aluminum carbonate mineral with the formula $(Sr,Ca)Al_2(CO_3)_2(OH)_4 \cdot H_2O$ (Jambor *et al.*, 1977). The type locality is the Francon Quarry, in Montreal, Quebec, Canada, but strontiodresserite is also reported to occur in France and Norway. It was first described by Jambor *et al.* (1977), with a Sr:Ca ratio of 4:1. Due to the small grain size, the diffraction data presented by Jambor *et al.* (1977) were limited to powder diffraction data.

Strontiodresserite is compositionally analogous to a small group of minerals which include dundasite $PbAl_2(CO_3)_2(OH)_4 \cdot H_2O$ (Cocco *et al.*, 1972), petterdite $PbCr_2(CO_3)_2(OH)_4 \cdot H_2O$ (Birch *et al.*, 2000), and dresserite $BaAl_2(CO_3)_2(OH)_4 \cdot H_2O$ (Jambor *et al.*, 1969). However, there is some disagreement in the literature as to whether strontiodresserite is isostructural with dundasite and dresserite. On the basis of the relationship between the elongations for the various directions of the optical axes, Jambor *et al.* (1977) suggested that dundasite, dresserite, and strontiodresserite are not isostructural. Roberts (1978) used long exposure X-ray precession single-crystal studies on two fibres of strontiodresserite to determine its space group. The systematic absences were consistent with either *Pbnm* or $Pbn2_1$ and, given the parallels reported by Cocco *et al.* (1972), Roberts (1978) concluded that strontiodresserite and dundasite are indeed isostructural.

The fine aggregate microstructure of these minerals makes single-crystal structure determination very difficult. The only published crystal structure amongst the group is for dundasite, where the researchers used the Weissenberg photographs of a multiple crystal (Cocco *et al.*, 1972). Despite the problematic sample, Cocco *et al.* (1972) successfully solved the structure and determined that dundasite contains a single water molecule per formula unit (f.u.).

Structure determination from powder diffraction (SDPD) data has developed significantly in recent years. Improvements in global optimization using real-space methods (Shankland and David, 2002) and more recently the application of the tangent formula (Coelho, 2007) to charge-flipping methods (Oszlányi and Süto, 2004) have greatly expanded

[a)]Author to whom correspondence should be addressed. Electronic mail: pamela.whitfield@nrc.gc.ca

Figure 1. (Color online) Optical image of strontiodresserite hemispheres embedded in the bulk silicocarbonatite sill rock. The hemispheres are approximately 1 mm in diameter.

the scope of SDPD. Together with improvements in data quality facilitated by developments in diffractometer instrumentation, SDPD has become accessible to a greater number of researchers. However, the results of a recent round robin suggest that it is still not a routine procedure (Le Bail and Cranswick, 2008).

II. EXPERIMENTAL AND DATA ANALYSIS

A. Sample preparation

The mineral of interest was presented as a number of 1 mm diameter, white, vitreous hemispheres (Figure 1) formed within vugs of a 10 cm sized piece of bulk silicocarbonatite sill rock from the Francon Quarry in Montreal, Quebec, Canada. Hemispheres were removed from the bulk under an optical microscope and an attempt was made to clean their surface of impurities. Of the six hemispheres obtained, four were gently crushed in ethanol using a mortar and pestle for X-ray diffraction analysis. Once dried, the powder was loaded into a 0.5 mm quartz capillary and the capillary sealed with wax before mounting in a standard brass capillary pin. One of the remaining hemispheres was lightly crushed and mounted onto a scanning electron microscope (SEM) stub using adhesive carbon film. The sample was examined in a Hitachi S4800 field emission SEM. Images and elemental analysis were obtained at 5 and 20 kV accelerating voltages, respectively.

B. X-ray data collection

The X-ray data were collected using a Bruker-AXS D8 diffractometer using Cu $K\alpha$ radiation with a focusing primary mirror and a Vantec PSD detector. Although the diffractometer was a θ-θ instrument, data were collected in the range from 9° to 140° 2θ with a fixed incident angle (the Debye-Scherrer geometry) using a 10° detector window. A variable count/step scheme was employed to improve counting statistics at high angle and produce more accurate results in the final Rietveld refinement (Madsen and Hill, 1994). The data collection scheme is given in Table I.

The data ranges were combined into a single file in "xye" format to retain the counting statistics information. All of the data analysis was done using the Bruker-AXS TOPAS 4.2 software (Bruker-AXS, 2008b). The least-squares indexing method (Coelho, 2003) was used to index the data from the first 25 peak positions determined through single-peak fitting. No background subtraction was necessary (including the capillary) to fit the background satisfactorily using a 15-term Chebyschev polynomial. This contrasts with the slight diffuseness in the powder diffraction data observed by Jambor *et al.* (1977) which they attributed to possible nonstoichiometry in carbonate and water content due to absorption from air.

TABLE I. Variable count-time data collection regime.

Start 2θ (deg)	End 2θ (deg)	Step size (deg)	Count time (s)
9.00	41.75	0.0142	2
41.75	74.50	0.0214	4
74.50	107.30	0.0285	8
107.30	140.00	0.0356	16

C. Structure solution and refinement

The ability to extract intensities out to low d spacings and the presence of a heavy atom (Sr) were positive indications that charge flipping (Oszlányi and Süto, 2004) might yield some of the atomic positions. The initial structure solution was accordingly attempted with a combination of charge-flipping method and tangent formula (Coelho, 2007). Low-density elimination (Shiono and Woolfson, 1992) was used to sharpen the resulting electron density.

Charge flipping produced sensible positions for the strontium, aluminum, and some oxygen atoms. Use of fixed positions for strontium and aluminum atoms in subsequent simulated annealing runs with data up to 80° 2θ greatly eased the difficulty of extracting a successful solution.

Rigid bodies consisting of regular AlO_6 octahedra and CO_3 triangles were used in conjunction with a "box interaction" penalty function such that at least eight oxygen atoms should be within 2.65 Å of a strontium atom. This model with six oxygen atoms around each aluminum and three around each carbon therefore contained initially 18 oxygen atoms/f.u., compared with 10 or 11 in the chemical formula. Merging of oxygen atoms approaching one another within 0.9 Å was accordingly implemented. Separate isotropic displacement parameters (B_{iso}) were used for the cations and anions. The oxygen atom for a water molecule was located on a Fourier difference map. The final refinement step involved all variable atom positions as well as individual B_{iso}.

The final refinement used the full data ranged up to 140° 2θ. The peak profiles were fitted using convolution-based peak profiles in combination with double-Voigt sample size-strain model (Balzar and Ledbetter, 1995). The simple axial divergence correction implemented in TOPAS (Bruker-AXS, 2008a) was used. Individual B_{iso} values were refined for the strontium, aluminum, carbon, and oxygen atoms, except for the equatorial AlO_6 oxygen atoms which were refined with an overall B_{iso}. The Sabine capillary absorption correction (Sabine *et al.*, 1998) was applied to the intensities. The linear absorption coefficient used in the correction included the contribution from the extraneous fluorite content.

https://doi.org/10.1154/1.3504496 Published online by Cambridge University Press

The wide 2θ range indicated that the application of the Debye-Scherrer capillary displacement 2θ correction (McCusker *et al.*, 1999) might be useful and was included in the input file as a user-defined macro.

D. Valence summation and location of hydrogen atoms

Bond valence sums were calculated using VaList (Wills, 2008). The bond-valence parameter for the mixed Sr-Ca site (2.088) was determined by applying percentage contribution from the refined site occupancies for Sr and Ca. A value of 0.37 was assumed for B, which is common to the bond-valence entries for Ca and Sr used as end members. Bond valence parameters for OH were taken from the 2006 version of bond-valence parameters maintained by I.D. Brown (2006a). No hydrogen atoms were included in the X-ray refinement of the data. A unique model for H positions in space group *Pnma* was then derived from crystal-chemical considerations as detailed in Sec. III A.

E. Modeling, DFT energy minimization, and structure stability

A crystal structure model combining the X-ray atom coordinates and the above hydrogen atoms was prepared and optimized by *ab initio* total energy minimization using the Vienna *Ab initio* Simulation Package (VASP) (Kresse, 1993; Kresse and Hafner, 1993) within the framework of density functional theory (DFT). Full occupancy by Sr of the (Sr,Ca) site was assumed. All modeling VASP input file preparation as well as output file interpretation was performed with Materials Toolkit (Le Page and Rodgers, 2005). The energy minimization scheme detailed by Mercier and Le Page (2008) was followed with a $4\times4\times4$ k mesh. Distorted models for the structure-stability test were prepared with the NUDGE utility (Le Page and Rodgers, 2006) in Materials Toolkit and optimized with VASP.

III. RESULTS AND DISCUSSION

A. The sample and its analysis

The sample under examination had been macroscopically identified as montroyalite, $Sr_4Al_8[(OH),F]_{26}(CO_3)_3 \cdot 10–11H_2O$ (Roberts *et al.*, 1986), a mineral also found in the Francon Quarry that typically occurs as small white hemispheres (similar to strontiodresserite) and coincidentally has the same Sr:Al ratio as strontiodresserite. The hemispherical nature of the material in question is apparent in the optical micrograph shown in Figure 1. The identity of the mineral was called into question when the powder diffraction was examined as the data did not resemble that expected from montroyalite (Roberts *et al.*, 1986). The possibility of a dehydration product of montroyalite was considered, but both the position and relative intensities of the reflections closely resembled those reported in the literature for strontiodresserite. Consequently, the structure solution process was started on the assumption that it was, in fact, strontiodresserite.

A small number of reflections from fluorite were visible and these were fitted as a secondary phase during the complete analysis process. Fluorite is not mentioned as a phase associated with strontiodresserite (Jambor *et al.*, 1977) but is associated with the fluorine-containing montroyalite (Roberts *et al.*, 1986). None of the closely associated minerals mentioned by Jambor *et al.* (1977), such as quartz and dawsonite, were present in the diffraction pattern.

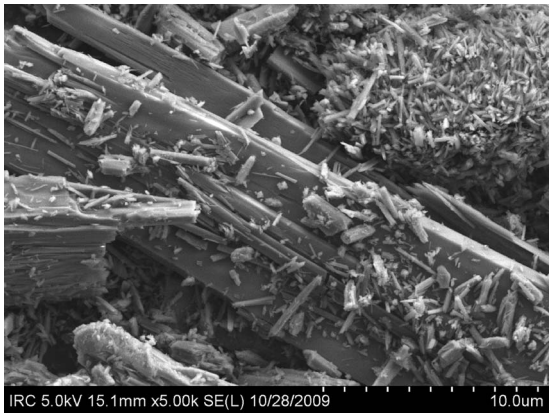

Figure 2. A SEM micrograph of a crushed strontiodresserite hemisphere.

Examination of the material by SEM yielded heavily fractured lathlike needles as shown in Figure 2. Lathlike crystals are consistent both with the observations by Jambor *et al.* (1977) on strontiodresserite and those of Roberts *et al.* (1986) on montroyalite including the "splintery fracture." EDX measurements yielded a Sr:Al atomic ratio of approximately 1:2. No signal from fluorine was detected either at 20 kV or when the voltage was lowered to optimize the detection of lighter elements, which is additional evidence that the sample was strontiodresserite as opposed to montroyalite.

B. Unit-cell analysis

The crystallinity of strontiodresserite was found to be quite good with distinct reflections visible all the way up to the limit of 140° 2θ as can be seen in the inset of Figure 3. Single peak fitting to obtain the first 25 to 30 reflections was

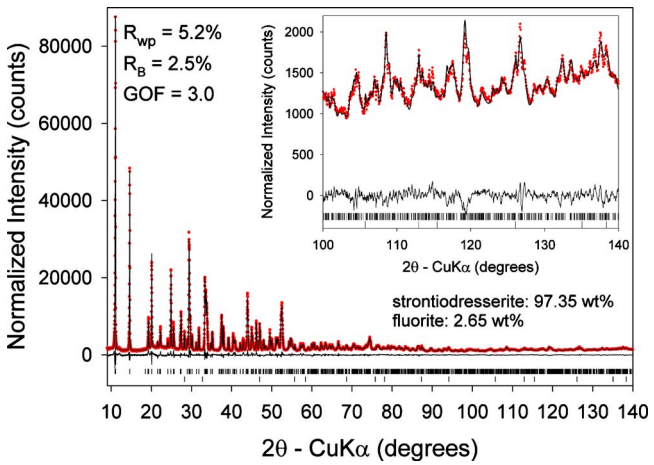

Figure 3. (Color online) Rietveld difference plot for the refinement of the strontiodresserite structure. The inset shows a blowup of the region between 100° and 140° 2θ.

https://doi.org/10.1154/1.3504496 Published online by Cambridge University Press

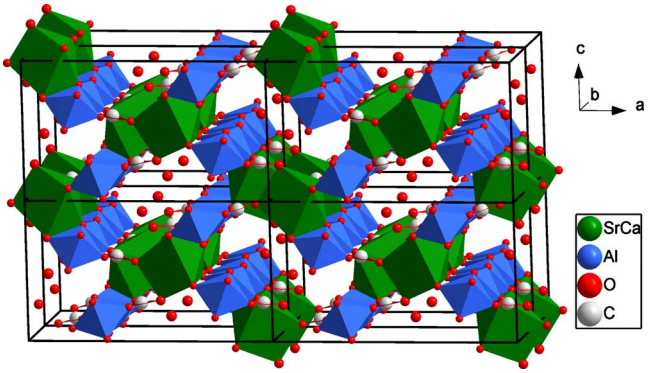

Figure 4. (Color online) Polyhedral representation of the experimental strontiodresserite crystal structure.

straightforward and 25 of those were used as input in the LSI indexing algorithm. Using a calculated lines to observed line ratio of 5, the first 70 solutions from the indexing in TOPAS gave the same orthorhombic lattice parameters with a=16.1, b=9.2, and c=5.6 Å, giving a very high confidence in the result. The first four solutions of the top 5 had the suggested space group $Pna2_1$ corresponding to the extinction symbol Pna-. Besides $Pna2_1$, the space group *Pnam* also belongs to the extinction symbol Pna-(Looijenga-Vos and Buerger, 2006), yielding effectively the same choice as that presented by Roberts (1978). The top solution had a GOF of 28.1 with a minimal zero point error. A Le Bail full pattern fit (Le Bail *et al.*, 1988) to the data ranging from 9° to 80° 2θ, including the fluorite secondary phase, yielded good fits in both $Pna2_1$ and *Pnam* (R_{wp}=5.0%). *Pnam* and *Pbnm* are alternate settings of the standard space group *Pnma* (No. 62).

C. Structure analysis

The first cycles of charge flipping yielded the strontium atom positions. Following cycles gave aluminum atom positions. The positions determined from the charge flipping accounted for the cell symmetry and identified the special position of the strontium atoms. Fixing the positions of the strontium and aluminum atoms in the simulated annealing assisted in finding the other atom positions relatively quickly. The oxygen atom of the water molecule was not subjected to any constraints, and took a little longer to locate reliably. The rigid-body octahedra used in the simulated annealing led to excess of oxygen atoms compared to the nominal stoichiometry. The partially merged oxygen atoms accordingly had to be consolidated in single sites for refinement upon removing the rigid-body constraints, leading to the expected stoichiometry.

A fourth-order spherical harmonics preferential orientation correction (Järvinen, 1993) was necessary to finalize the refinement. The application of this correction did not alter the overall structure but greatly improved the geometry of the carbonate ions and significantly improved the fit. The refined B_{iso} of the Sr appeared to be sensitive to the preferential orientation correction, and the value increased after the application of the spherical harmonics. Orientation of a powder in a capillary is suggestive of needle or lath-shaped crystallites, which has been reported previously with strontiodresserite (Jambor *et al.*, 1977) and can be seen in Figure 2.

Although a Fourier difference map confirmed the location of the water oxygen atom, no additional water molecules were found and none of the hydrogen atoms could reliably be located by X-rays. As expected, the capillary displacement was minimal (x=+0.03 mm and y=+0.04 mm) but did improve the R_{wp} residual slightly.

The final refinement was carried out in the standard setting for space group number 62, which is *Pnma*. The cell and structure can be transformed to the *Pbnm* cell by the application of a *cab* matrix transformation for comparison with the previously described structure of dundasite (Cocco *et al.*, 1972). The final refined lattice parameters in *Pnma* were a=16.0990(7), b=5.6133(3), and c=9.1804(4) Å, with Z=4. The fit to the experimental data was very good as shown in Figure 3, with a R_{wp} value of 5.2%. The density of strontiodresserite calculated with those cell parameters is 2.66 g/cm^3, which compares quite well with the measured value of 2.71 g/cm^3 (Jambor *et al.*, 1977) given that the refined Ca content on the Sr site is very slightly lower at 19.3% than the nominal value of 20%.

TABLE II. Refined experimental atomic coordinates for strontiodresserite.

Atom	Wyckoff position	x	y	z	Occ	B_{iso} (Å^2)
Sr	4c	0.4146(6)	$\frac{3}{4}$	0.4740(1)	0.807(7)	6.0(12)
Ca					0.193(7)	
Al	8d	0.2039(1)	0.5029(6)	0.6693(3)	1	1.34(6)
C1	4c	0.5499(9)	$\frac{3}{4}$	0.7516(14)	1	3.1(2)
C2	4c	0.3540(8)	$\frac{1}{4}$	0.5830(15)	1	3.1(2)
O1	4c	0.2180(4)	$\frac{1}{4}$	0.8038(7)	1	0.99(8)
O2	4c	0.1620(3)	$\frac{1}{4}$	0.5402(8)	1	0.99(8)
O3	8d	0.0889(3)	0.5472(11)	0.7388(5)	1	1.2(1)
O4	4c	0.2428(3)	$\frac{3}{4}$	0.7822(7)	1	0.99(8)
O5	8d	0.3165(3)	0.4505(9)	0.5953(5)	1	1.1(1)
O6	4c	0.1859(3)	$\frac{3}{4}$	0.5305(8)	1	0.99(8)
O7	4c	0.4716(4)	$\frac{3}{4}$	0.7348(7)	1	1.7(2)
O8	4c	0.4271(4)	$\frac{1}{4}$	0.5437(8)	1	1.2(2)
O9w	4c	0.5375(4)	$\frac{3}{4}$	0.1007(8)	1	2.0(2)

https://doi.org/10.1154/1.3504496 Published online by Cambridge University Press

TABLE III. Bond valence sums for the strontiodresserite structure. The underlined oxygen atoms indicate the hydroxide oxygens.

Atom	BVS
Sr1(80.7% Sr+19.3% Ca)	1.9
Al1	2.7
C1	4.0
C2	4.2
O1	1.2
O2	0.8
O3	1.9
O4	1.1
O5	2.1
O6	0.9
O7	1.7
O8	2.1

TABLE IV. *Ab initio* optimized atomic coordinates for strontiodresserite.

Atom	Wyckoff position	*x*	*y*	*z*
Sr	4*c*	0.414 16	$\frac{3}{4}$	0.475 73
Al	8*d*	0.204 17	0.501 75	0.672 22
C1	4*c*	0.550 58	$\frac{3}{4}$	0.751 32
C2	4*c*	0.353 98	$\frac{1}{4}$	0.581 53
O1	4*c*	0.214 53	$\frac{1}{4}$	0.805 53
O2	4*c*	0.165 95	$\frac{1}{4}$	0.547 08
O3	8*d*	0.090 89	0.547 21	0.740 19
O4	4*c*	0.241 84	$\frac{3}{4}$	0.786 13
O5	8*d*	0.315 47	0.451 26	0.598 42
O6	4*c*	0.187 91	$\frac{3}{4}$	0.534 21
O7	4*c*	0.472 32	$\frac{3}{4}$	0.734 42
O8	4*c*	0.431 01	$\frac{1}{4}$	0.545 28
O9w	4*c*	0.541 02	$\frac{3}{4}$	0.097 22
H1	4*c*	0.256 16	$\frac{1}{4}$	0.887 56
H2	4*c*	0.105 65	$\frac{1}{4}$	0.534 20
H4	4*c*	0.280 46	$\frac{3}{4}$	0.869 35
H6	4*c*	0.132 28	$\frac{3}{4}$	0.484 16
H9w	8*d*	0.529 87	0.610 27	0.158 86

D. Structure description

The structure consists of corrugated chains extending along the *b* axis. Those chains are made of edge-sharing AlO_6 octahedra, as shown in Figure 4. Four coplanar oxygen atoms are shared in this way in an equatorial plane of each Al atom, while two axial oxygen atoms lie perpendicular to that plane. Next to each of the AlO_6 chains, the strontium atom shares edges with two AlO_6 octahedra. In the *b* direction the irregular-shaped SrO_9 polyhedra alternate with the carbonate ions which are corner sharing with two axial AlO_6 oxygen atoms and share an oxygen atom with the opposite SrO_9. The carbonate ions effectively tie together the two Al/Sr/O layers in the unit cell. The water molecules are located in channels running along the *b* direction and are not coordinated directly with any of the cations. The position of the oxygen atom does suggest the possibility of hydrogen bonding with oxygen atoms in the polyhedral network. Bond valence analysis confirmed that the hydroxyl oxygen atoms are O1, O2, O4, and O6, which are the equatorial oxygen atoms of the AlO_6 octahedra. Table II lists the atomic coordinates from Rietveld refinement of nonhydrogen atoms in space group *Pnma*. Table III shows the results of bond-valence summation using atom coordinates in Table II.

E. Location of hydrogen atoms

The fact that O9w could be refined to a B_{iso} of 2.0(2) with full oxygen occupancy is an indication that water molecules are strongly bound with just one scheme of hydrogen bonds, and that an ordered hydrogen-bond scheme most probably exists in strontiodresserite. Examination of experimental O-O approaches for O9w indicates that only three oxygen atoms, O3 (×2) and O6 at respective distances of 2.92 and 2.68 Å, can possibly be involved in hydrogen bonding with O9w. The next shortest distance of 3.19 Å is too long to be part of a significant hydrogen bond [see, e.g., Figure 1 in Ferraris and Ivaldi (1988)]. From bond-valence summation, O6 is known to be an OH group, thus indicating an O6-H6…O9w hydrogen bond. The two short approaches between O9w and O3 are then the two O9w-H9…O3 hydrogen bonds of the water molecule. The remaining OH groups at O1, O2, and O4 are all bonded to two Al^{3+} ions. Simple electrostatic field considerations then suggest an initial location of corresponding hydroxyl hydrogen atoms on the line joining the midpoint between the two Al^{3+} ions and the oxygen atom away from the aluminum ions. Qualitatively, this hydrogen-bond scheme is unique in space group *Pnma*. Initial O-H distances were assumed to be 1 Å.

F. DFT energy minimization of strontiodresserite and dundasite

DFT energy minimization by adjustment of atom coordinates of this model in the fixed experimental cell proceeded smoothly, without any large drift of the proposed hydrogen atoms or of the framework atoms, a strong indication of a sensible initial model. Table IV lists all atom coordinates, including hydrogen atoms after DFT optimization with VASP in space group *Pnma*. Selected bond distances are shown in two columns in Table V for easy comparison of X-ray and *ab initio* VASP results. Bond angles from *ab initio* VASP results pertaining to the hydrogen bonding are given in Table VI. The bonds involving hydrogens from the DFT model are shown graphically in Figure 5 for easy interpretation of Tables IV–VI. There are no large discrepancies from expected values including all optimized O-H distances of about 1 Å. As expected the agreement between experimental and DFT bond lengths tends to be better with the heavier elements as they are more easily localized with X-ray powder diffraction data. From Table VI, the H-O-H angle in the water molecule as well as H…O-H angles are all reasonably close to tetrahedral angles. The only deviation from an ideal model for a textbook seems to be that the O9w-H9w…O3 angle deviates from 180°. We consider this to be a minor imperfection because the H9w…O3 hydrogen bond is rather weak. H9w is accordingly pointing to an electrostatically negatively charged region on the wall of a wide channel rather than establishing a strong hydrogen bond with O3, which ought to be in straight line. We tested the energy of plausible disordered hydrogen-bond models at O9w, with lower symmetry. All those that did not revert to the above

https://doi.org/10.1154/1.3504496 Published online by Cambridge University Press

TABLE V. Selected bond distances derived from the refinement of the experimental data and the DFT-optimized structure.

Bond pair	Experimental (298 K) bond distance (Å)	DTF (0 K) bond distance (Å)
Sr1-O1	2.645(6)	2.595
Sr1-O3	2.729(5)	2.732
Sr1-O5	2.562(5)	2.570
Sr1-O7	2.564(7)	2.553
Sr1-O8	2.554(6)	2.500
Al1-O1 (equatorial)	1.895(5)	1.867
Al1-O3 (axial)	1.974(5)	1.944
C1-O3	1.304(9)	1.313
C1-O7	1.27(2)	1.269
C2-O5	1.283(8)	1.298
C2-O8	1.23(1)	1.284
O9w-H9w	···	0.984
H9w-O3	···	2.262
H9w-O7	···	2.247
H6-O9w	···	1.648
H1-O6	···	1.620
H4-O2	···	1.846

scheme failed to reduce the total energy and yielded atomic coordinates for O9w that differed from those found experimentally.

G. Space-group choice for strontiodresserite and dundasite

The success of the structure solution in a particular space group from diffraction intensities, as well as its DFT optimization in that space group, does not prove that the correct structure is not actually distorted with a lower symmetry. We accordingly tested the *ab initio* stability of the final tabulated crystal structure of strontiodresserite by creating models of it in *P*1, introducing random tiny individual distortions into all atom coordinates and all cell vectors. Total energy minimization will promptly return this randomly distorted crystal structure to its initial configuration and symmetry if it is stable. In contrast, an unstable model will converge to a new configuration with lower energy and lower symmetry. The test performed with the NUDGE utility (Le Page and Rodgers, 2006) on the strontiodresserite *P*1 model confirmed that the *Pnma* model of strontiodresserite is stable and lowering

TABLE VI. Selected bond angles from the DTF-optimized structure.

Atom grouping	Bond angle (deg)
O1-H1…O6	172
O4-H4…O2	169
O6-H6…O9w	180
O9w-H9w…O3	131
O9w-H9w…O7	166
H9w-O9w-H9w	106
H6…O9w-H9w	115
H1…O6-H6	97
H4…O2-H2	111

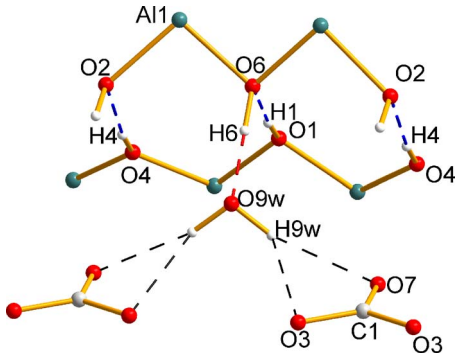

Figure 5. (Color online) The hydrogen bonding network in strontiodresserite.

the symmetry is not necessary. The same test, repeated with the literature structure of dundasite combined with hydrogen atoms from strontiodresserite, confirmed the structure and symmetry of dundasite as reported by Cocco *et al.* (1972).

H. Complementarity of powder methods, valence summation, and DFT optimization

This study illustrates the fact that the combination of laboratory X-ray Rietveld profile analysis with valence summation and *ab initio* methods can, in a number of cases, reliably elucidate crystal structures of a complexity that used to require X-ray single-crystal diffraction. As shown here, this possibility opens new perspectives with samples that can be obtained in powder form only. For oxides, bond-valence summation (Brown, 2006b) provides a powerful check of the validity of the crystal structure, but *ab initio* optimization provides several additional and very stringent checks about the correctness of the structure model. The first such check is that stress calculated *ab initio* using experimental cell parameters was verified here to be small and uniform. With VASP, this stress is usually calculated as a small negative and essentially isotropic pressure, in part because *ab initio* calculations are performed at 0 K temperature and also due to tiny imperfections in the numerical representation of quantum-calculated core electron density. A second test is that calculated optimized atom coordinates for atoms should actually match the experimentally determined atom positions. This test is particularly powerful in cases like here, where some atoms were located experimentally while others are deduced from crystal-chemical considerations: a wrong assignment of hydrogen atoms would have repercussions on hydroxyl and water oxygen positions. Verification of the match of coordinates within least-squares uncertainties then validates both the framework architecture and the hydrogen-bond scheme deduced from it. The third test is that of the stability of the optimized structure model as explained previously. This test validated here the use of space group *Pnma* for the structure solution, demonstrating that a lower symmetry was not required.

IV. CONCLUSION

The structure of strontiodresserite has been determined from laboratory powder diffraction data using a combination

https://doi.org/10.1154/1.3504496 Published online by Cambridge University Press

of charge-flipping and simulated annealing techniques. The crystal structure is orthorhombic and has been described in *Pnma*, with two chains of AlO_6 octahedra along the *b* direction linked by irregular SrO_9 polyhedra and carbonate ions. The water molecule lies in a channel that runs parallel to the *b* axis. This study confirms the isostructural relationship between strontiodresserite and dundasite proposed by Roberts (1978). The hydroxyl and water oxygens were identified using bond-valence sums. A unique model of hydrogen atoms was then deduced from crystal chemistry and optimized by *ab initio* DFT energy minimization. The stability of the resulting *Pnma* strontiodresserite structure and that of the corresponding dundasite structure were then demonstrated using *ab initio* methods. Strontiodresserite and dundasite are isostructural in space group *Pnma*, basically as described by Cocco *et al.* (1972) albeit in *Pbnm*, including their hydrogen-bond network established here.

Balzar, D. and Ledbetter, H. (**1995**). "Accurate modelling of size and strain broadening in the Rietveld refinement: The 'double-Voigt' approach," Adv. X-Ray Anal. **38**, 397–404.

Birch, W. D., Kolitsch, U., Witzke, T., Nasdala, L., and Bottrill, R. S. (**2000**). "Petterdite, the Cr-dominant analogue of dundasite, a new mineral species from Dundas, Tasmania, Australia and Callenberg, Saxony, Germany," Can. Mineral. **38**, 1467–1476.

Brown, I. D. (**2006a**). bvparm2006.cif ⟨www.ccp14.ac.uk⟩.

Brown, I. D. (**2006b**). *The Chemical Bond in Inorganic Chemistry. The Bond Valence Model IUCr Monographs on Crystallography* (Oxford University Press, Oxford).

Bruker-AXS (**2008a**). *DIFFRACPlus TOPAS: TOPAS 4.2 Technical Reference (Computer Software)* (Bruker-AXS GmbH, Karlsruhe, Germany).

Bruker-AXS (**2008b**). *DIFFRACPlus TOPAS: TOPAS 4.2 User Manual. (Computer Software)* (Bruker-AXS GmbH, Karlsruhe, Germany).

Cocco, G., Fanfini, L., Nunzi, A., and Zanazzi, P. F. (**1972**). "The crystal structure of dundasite," Miner. Mag. **38**, 564–569.

Coelho, A. A. (**2003**). "Indexing of powder diffraction patterns by iterative use of singular value decomposition," J. Appl. Crystallogr. **36**, 86–95.

Coelho, A. A. (**2007**). "A charge flipping algorithm incorporating the tangent formula for solving difficult structures," Acta Crystallogr., Sect. A: Found. Crystallogr. **63**, 400–406.

Ferraris, G. and Ivaldi, G. (**1988**). "Bond valence vs bond length in O…O hydrogen bonds," Acta Crystallogr., Sect. B: Struct. Sci. **44**, 341–344.

Jambor, J. L., Fong, D. G., and Sabina, A. P. (**1969**). "Dresserite, the new barium analogue of dundasite," Can. Mineral. **10**, 84–89.

Jambor, J. L., Sabina, A. P., Roberts, A. C., and Sturman, B. D. (**1977**). "Strontiodresserite, a new Sr-Al carbonate from Montreal Island, Quebec," Can. Mineral. **15**, 405–407.

Järvinen, M. (**1993**). "Application of symmetrized harmonics expansion to correction of the preferred orientation effect," J. Appl. Crystallogr. **26**, 525–531.

Kresse, G. (**1993**). "Ab initio molekular dynamik für flüssige metalle," Ph.D. thesis, Technische Universität, Wien, Austria.

Kresse, G. and Hafner, J. (**1993**). "*Ab initio* molecular dynamics for open-shell transition metals," Phys. Rev. B **48**, 13115–13118.

Le Bail, A. and Cranswick, L. M. D. (**2008**). SDPDRR-3: Structure determination by powder diffractometry round robin 3 ⟨http://cristal.org/SDPDRR3/results/index.html⟩.

Le Bail, A., Duroy, H., and Fourquet, J. L. (**1988**). "Ab-initio structure determination of $LiSbWO_6$ by X-ray powder diffraction," Mater. Res. Bull. **23**, 447–452.

Le Page, Y. and Rodgers, J. R. (**2005**). "Quantum software interfaced with crystal structure databases: Tools, results and perspectives," J. Appl. Crystallogr. **38**, 697–705.

Le Page, Y. and Rodgers, J. R. (**2006**). "Low energy models from scratch: Application to SiNF," Comput. Mater. Sci. **37**, 537–542.

Looijenga-Vos, A. and Buerger, M. J. (**2006**). "Space-group determination and diffraction symbols," *International Tables for Crystallography*, edited by Th. Hahn (International Union for Crystallography, Chester, UK), Vol. A, p. 44.

Madsen, I. C. and Hill, R. J. (**1994**). "Collection and analysis of powder diffraction data with near-constant counting statistics," J. Appl. Crystallogr. **27**, 385–392.

McCusker, L. B., Von Dreele, R. B., Cox, D. E., Louer, D., and Scardi, P. (**1999**). "Rietveld refinement guidelines," J. Appl. Crystallogr. **32**, 36–50.

Mercier, P. H. J. and Le Page, Y. (**2008**). "Kaolin polytypes revisited ab initio," Acta Crystallogr., Sect. B: Struct. Sci. **64**, 131–143.

Oszlányi, G. and Süto, A. (**2004**). "Ab initio structure solution by charge flipping," Acta Crystallogr., Sect. A: Found. Crystallogr. **60**, 134–141.

Roberts, A. C. (**1978**). "Geological Survey of Canada, Current Research, Part B," 78-1B, 180.

Roberts, A. C., Sabina, A. P., Bonardi, M., Jambor, J. L., Ramik, R. A., Sturman, B. D., and Carr, M. J. (**1986**). "Montroyalite, a new hydrated Sr-Al hydroxycarbonate from the Francon Quarry, Montreal, Quebec," Can. Mineral. **24**, 455–459.

Sabine, T. M., Hunter, B. A., Sabine, W. R., and Ball, C. J. (**1998**). "Analytical expressions for the transmission factor and peak shift in absorbing cylindrical specimens," J. Appl. Crystallogr. **31**, 47–51.

Shankland, K. and David, W. I. F. (**2002**). "Global optimization strategies," *Structure Determination from Powder Diffraction Data*, edited by W. I. F. David, K. Shankland, L. B. McCusker, and Ch. Baerlocher (Oxford University Press, Oxford, UK), pp. 252–285.

Shiono, M. and Woolfson, M. M. (**1992**). "Direct-space methods in phase extension and phase determination. 1. Low-density elimination," Acta Crystallogr., Sect. A: Found. Crystallogr. **48**, 451–456.

Wills, A. S. (**2008**). VaList (Computer Program) ⟨www.ccp14.ac.uk⟩.